

Online search of unknown terrains using a dynamical system-based path planning approach

Karan Sridharan
Department of Mechanical Engineering
Wichita State University
Wichita, Kansas 67260
Email: kxsridharan@shockers.wichita.edu

Zahra Nili Ahmadabadi¹
Department of Mechanical Engineering
San Diego State University
San Diego, California 92182
Email: zniliahadabadi@sdsu.edu

Jeffrey Hudack
Information Directorate
Air Force Research Laboratory
Rome, NY 13441
Email: jeffrey.hudack@us.af.mil

ABSTRACT

Surveillance and exploration of large environments is a tedious task. In spaces with limited environmental cues, random-like search appears to be an effective approach as it allows the robot to perform online coverage of environments using a simple design. One way to generate random-like scanning is to use nonlinear dynamical systems to impart chaos into the robot's controller. This will result in generation of unpredictable but at the same time deterministic trajectories, allowing the designer to control the system and achieve a high scanning coverage. However, the unpredictability comes at the cost of increased coverage time and lack of scalability, both of which have been ignored by the state-of-the-art chaotic path planners. This study introduces a new scalable technique that helps a robot to steer away from the obstacles and cover the entire space in a short period of time. The technique involves coupling and manipulating two chaotic systems to minimize the coverage time and enable scanning of unknown environments with different properties online. Using this technique resulted in 49% boost, on average, in the robot's performance compared to the state-of-the-art planners. While ensuring unpredictability in the paths, the overall performance of the chaotic planner remained comparable to optimal systems.

KEYWORDS: Autonomous robot, Path planning, Unpredictable search, Dynamical systems, Unknown environments.

¹ Corresponding author

NOMENCLATURE

A	Arnold system's parameter	CT	Time for 90% coverage rate
B	Arnold system's parameter	tc	Total coverage rate
C	Arnold system's parameter	tc_{new}	Total coverage rate at $t + \Delta t$
c	Coverage criterion factor	tc_{old}	Total coverage rate at t
$coord_{obs}$	Coordinate matrix of obstacles	t_h	Maximum number of attempts to avoid an obstacle
$coord_{boundary}$	Coordinate matrix of the map boundaries	T_p	Matrix storing all trajectory points
dc	Desired coverage rate	TP_{DS-R}	Temporary matrix of Arnold DS and robot coordinates
d	Distance between the robot's current position and a zone's midpoint	$TP_{DS-R-logistic}$	Temporary matrix of Logistic map initial DS and robot's coordinates
e_p	Error tolerance of trajectory points	$TP_{scaled-R}$	Temporary matrix of scaled robot coordinates
f_o	Obstacle/boundary offset factor	t_{TR}	Time taken to travel between two zones
f	Scaling factor	$upper$	Upper boundary
i, j	Incremental index	v	Robot's velocity
DS_{index}	Index for each DS coordinate	x_n, x_{n+1}	Coordinates of Logistic map system at current and next iterations
$left$	Left boundary	$\hat{X}_{n+1}, \hat{Y}_{n+1}$	Relative coordinates of Logistic map system in next iteration
$lower$	Lower boundary	X'_{n+1}, Y'_{n+1}	Mapped coordinate of Logistic map system in next iteration
l_{zone}	List of zones with their respective properties	$X(t), Y(t)$	Robot coordinates mapped from Arnold system
M	Column coordinates	$X_n, Y_n,$ X_{n+1}, Y_{n+1}	Robot coordinates mapped from Logistic map system in current (n) and next ($n+1$) iterations
m	Number of logistic map trajectory points on constructed path between two zones	X_{end}, Y_{end}	Zone's Midpoint coordinates
N	Row coordinates	$[X, Y]$	Trajectory matrix
n	Coordinate index number	$[\hat{X}, \hat{Y}]$	Relative trajectory matrix
n_{iter}	Number of iterations	$[X', Y']$	Mapped trajectory matrix
n_h	Number of attempts to avoid an obstacle	$x(t), y(t), z(t)$	Coordinates of Arnold system
n_{map}	Last row index in mapped matrix $[X', Y']$	Δt	Time step
$n_{TP_{DS-R}}$	Last row index in TP_{DS-R}	$\Delta t_{adaptive}$	Adaptive time step
$n_{TP_{DS-R-logistic}}$	Last row index in $TP_{DS-R-logistic}$	$\Delta t_{constant}$	Constant time step
r	Logistic map system's parameter	Δn_h	Change in n_h
$right$	Right boundary	θ	Mapping variable
t	Time	ρ	Zone's coverage density

1 INTRODUCTION

Smart mobile robots with coverage path planning (CPP) algorithms have been increasingly employed in various applications, ranging from household [1, 2] to surveillance and search [3-9] and agricultural [10-15]. CPP algorithms construct a path for the robot to visit every area in a map and simultaneously avoid obstacles. Among existing CPP algorithms, the chaotic path planning is one of the most upcoming methods useful in surveillance and exploration applications. In surveillance missions, the robot should perform an online scan of an uncertain environment without the need for the map and in minimum amount of time to find an object/target, while avoiding the obstacles and adversaries in their path. Due to their deterministic nature and the possibility of being controlled by their designer, the chaotic path planners have the potential to fulfill these requirements while remaining unpredictable to adversaries.

To generate chaotic trajectories, the nonlinear dynamical systems (DS) are used to induce chaos into the robot's controller. Nakamura and Sekiguchi [16] demonstrated that chaotic path planning is more effective than random-walk, which restricts the continuity in the robot's motion and often results in uneven density of coverage distributed across the space. With chaotic path planning algorithms, the robot was able to generate continuous trajectories and examine the entire area of the map more efficiently.

A major disadvantage of using chaotic dynamical systems for CPP is that they increase coverage time since most chaotic systems generate undispersed points across the map, and research has focused on manipulating chaotic path planning algorithms [17-20] to increase the dispersal of trajectory points across the map. Examples of chaos manipulation techniques include: arccosine and arcsine transformation [20] and random number generators [21]. The coverage rate criterion [16, 21-26] was used by most studies to examine the efficiency of chaotic algorithms while the coverage time was neglected. One challenge that has not been addressed by previous studies is scalability, which allows adaptation to new environments with different properties (e.g., size) and to cover them in finite time.

In this work, three chaos control methods were combined to enhance coverage rate and minimize coverage time in unknown environments: (1) orientation control, (2) map zoning, and (3) system scaling. Orientation control guides the robot to change direction and cover new cells in adjacent regions, map zoning guides the robot to regions that display less coverage, and system scaling allows varying the coverage density based on the sensor range and environment size. The first two chaos control techniques were introduced in [27] where properties of the continuous Lorenz system and the discrete Hénon map system were combined to achieve fast coverage in an environment with no obstacles, but were not as well capable to adapt to environments with unknown obstacles and to variations in the sensing range (SR) and the environment size.

To address these issues, we introduce a new hybrid system which includes the continuous Arnold system and the discrete Logistic map system, leading to relatively faster coverage. We also introduce an obstacle avoidance technique which enhances the scalability of the path planner in environments with unknown obstacles. Using a combination of these techniques, the robot will be able to prevent repeated coverage and achieve the desired coverage rate in unknown environments quickly.

The rest of the paper is organized as follows: Section 2 introduces the chaotic systems and how they are integrated to construct the robot's trajectory. Section 3 describes the path planning strategy and chaos control techniques. This is followed by Section 4 which discusses the obstacle/boundary avoidance methods. Section 5 presents the simulation results of the robot scanning an unknown environment with and without obstacles. Finally, Section 6 concludes the paper and highlights the future work.

2 CHAOTIC DYNAMICAL SYSTEMS AND THEIR INTEGRATION IN MOBILE ROBOT

Chaotic dynamical systems are represented as continuous [16, 22, 28-30] or discrete [18-20, 31, 32] systems, with the Arnold (see Eq. (1)) [16] and Logistic map (see Eq. (2)) [20] systems yielding minimal coverage time, described with the following equations:

$$\begin{aligned} dx(t)/dt &= A \sin z(t) + C \cos y(t) \\ dy(t)/dt &= B \sin x(t) + A \cos z(t) \end{aligned} \quad (1)$$

$$dz(t)/dt = C \sin y(t) + B \cos x(t)$$

$$x_{n+1} = rx_n(1-x_n) \quad (2)$$

where $x(t)$, $y(t)$, and $z(t)$ are the DS coordinates; A , B and C are the Arnold system parameters; x_n and x_{n+1} are the Logistic map system coordinate points for the current and new states, respectively; and r is the Logistic system parameter. To be considered chaotic, nonlinear dynamical systems should possess the following characteristics: (1) sensitivity to initial conditions (ICs), and (2) topological transitivity. In this work, we use the following ICs for the Arnold system: $x_0 = 0$, $y_0 = 1$, and $z_0 = 0$. As for the Logistic map system, the chosen IC was $x_0 = 0.1$. Based on analysis of the parameter space, the Arnold system parameters are [16]: $A = 0.5$, $B = 0.25$ and $C = 0.25$. For the Logistic map system, the parameter $r = 4$ was selected [20]. Fig. 1 shows the 3-D chaos attractor of the Arnold system obtained using the above-mentioned parameters. As the Logistic map is a 1-D system, its chaos attractor does not exist, and is therefore not included here.

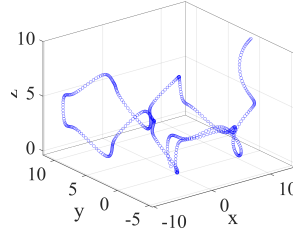


Fig 1. 3-D Chaos attractor for the Arnold system.

The algorithm maps the DS coordinates into the robot's kinematic equation, i.e., the DS coordinates replace the robot's orientation. Fig. 2 depicts the two-wheel differential drive mobile robot used in this study. The robot comprises of two active fixed wheels and one passive caster wheel and it is subject to a non-holonomic constraint. Eqs. (3) and (4) represent the mapping process for the Arnold and Logistic map systems, as suggested by [22] and [20], respectively:

$$dX(t)/dt = v \cos(x(t)) \quad (3)$$

$$dY(t)/dt = v \sin(x(t))$$

$$\omega(t) = d\theta(t)/dt = dx(t)/dt$$

$$\theta_n = \pi x_n \pm \frac{\pi}{2} \quad (4)$$

$$X_{n+1} = X_n + \Delta t v \cos \theta_n$$

$$Y_{n+1} = Y_n + \Delta t v \sin \theta_n$$

$$\omega_n = (\theta_{n+1} - \theta_n)/\Delta t$$

In Eq. (3), $X(t)$ and $Y(t)$ are the robot's coordinates, v is the robot's velocity, dt or Δt is the time step, and $x(t)$ is one of the Arnold system coordinates mapped into the robot's kinematic equations. In the following sections of this study, the robot coordinates are referred to as the trajectory points. It is important to note that the 3-D Arnold system has been used in this study (see Eq. (1)) and therefore any of the other two DS coordinates ($y(t)$ or $z(t)$) can replace $x(t)$ in Eq. (3) to perform the mapping.

In Eq. (4), X_n and Y_n are the coordinates of the current states, X_{n+1} and Y_{n+1} are the coordinates of the new states, and θ_n is a mapping variable that translates the DS coordinates to the robot's coordinate (i.e., robot's orientation). The discrete systems usually tend to drive the robot in only one direction, the first relation in Eq. (4) is meant to prevent this problem by switching the sign next to the phase angle and directing the robot to move in all directions. For instance, if the robot is heading close to the left boundary, the algorithm will set θ_n equal to $\pi x_n - \pi/2$ and steer the robot to navigate toward the right boundary. If the opposite occurs, the algorithm will set θ_n equal to $\pi x_n + \pi/2$ and steer the robot to navigate toward the left boundary.

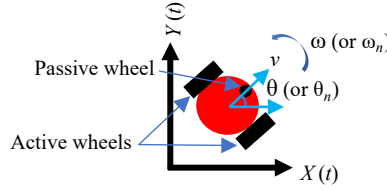


Fig 2. A schematic of mobile robot's motion on a plane.

3 PATH PLANNING STRATEGY AND CHAOS CONTROL TECHNIQUES

Our objective is to reduce repetitive coverage and eliminate lack of scalability, both of which will lead to extended coverage time. To address these, we employ: (1) an orientation control technique which guides the robot to cover less-visited adjacent regions, (2) a map zoning technique to direct the robot to less-visited distant regions, and (3) a system scaling technique to reduce repetitive coverage and adapt to changes in the robot's sensing range and environment size. In what follows, cells refer to small segments in the map while zones indicate larger segments.

We make the following simplifying assumptions to reduce the computational difficulty of the simulation task: (1) the environments are square rooms with boundaries on all sides; (2) the robot's velocity is constant 1 m/s to simulate a small two-wheeled differential drive robot; (3) three different relatively large world sizes (50 m \times 50 m, 100 m \times 100 m, 200 m \times 200 m) are examined; (4) the sensing range determines the cell dimensions in each environment, e.g., cell dimensions of 4 m \times 4 m correspond to four meters sensing range; (5) all systems are run to achieve the desired coverage rate of 90%, (6) in simulation, the robot uses the coordinate matrix of obstacles ($coor_{obs}$) and map boundaries ($coor_{boundary}$) to detect obstacles' and walls' boundaries, respectively, though in real-life, the sensors are used for this purpose; and (7) the robot can start the coverage task from any point in the environment, as long as the selected point is not occupied by an obstacle. In this study, the selected starting point for a robot scanning a map with zero and one obstacle was $X(t) = 0.5$ m and $Y(t) = 0.5$ m. For the environment with four and five obstacles, the robot's starting points were as follows: $X(t) = 15$ m and $Y(t) = 5$ m in a 50 m \times 50 m; $X(t) = 30$ m, $Y(t) = 10$ m in a 100 m \times 100 m environment, and $X(t) = 60$ m, $Y(t) = 20$ m in a 200 m \times 200 m environment. Here, the starting point indicates the coordinates of the robot at the beginning of the coverage task.

The algorithm (Algorithm 1) uses the Arnold system as the primary system to scan the environment, continuing until the desired coverage (dc) is achieved. At each iteration, it invokes the SystemScaler function (Algorithm 3) to generate trajectory points for the robot using the Arnold system to scan the area and adds the generated points (stored under temporary matrix $TP_{scaled-R}$) to the storage matrix T_p . The need for scaling and its level is determined by the scaling factor (f), which indicates to the SystemScaler to scale the trajectory points before returning them. Using the data stored under the matrix T_p , it updates the coverage rate (tc) and time (t), respectively.

To determine whether to focus on orientation or zoning, we use the following criterion:

$$\frac{\text{New cells visited in } [t-\Delta t : t]}{\text{Total of new and repetitive cells visited in } [t-\Delta t : t]} \geq c \left[\frac{\text{Total unvisited cells in } [0 : t-\Delta t]}{\text{Total number of cells}} \right] \quad (5)$$

which indicates if the current trajectory is recently successful in visiting new cells in the current zone. Otherwise, the robot should leave the current trajectory and zone and travel to another zone where it starts a new trajectory. In this case, Algorithm 1 calls the function *MapZoning* (Algorithm 2) in line 23; this function finds the next best zone for coverage and generates a direct chaotic path between the current robot's position and the midpoint of the new zone using the Logistic map system. Algorithm 4 is used to find an obstacle free path to the new zone. Once arrived at the new zone, Algorithm 3 (*SystemScaler*) will generate n new trajectory points for the robot to continue the coverage task in the new zone.

Algorithm 1: Chaotic path planning algorithm

Inputs: $A, B, C, r, TP_{DS-R}, TP_{DS-R-logistic}, f_o, f, n_h, \Delta n_h, n_{iter}, coor_{boundary}, c, dc, e_p, le, t_h, v, \Delta t_{constant}, \Delta t_{adaptive}, t$
Outputs: tc, t

- 1 Initialize DS_{index}
- 2 $tc \leftarrow 0$
- 3 $T_p \leftarrow \emptyset$
- 4 $tc_{new} \leftarrow 0$
- 5 **while** ($tc < dc$) **do**
- 6 $tc_{old} \leftarrow tc_{new}$
- 7 $\{TP_{DS-R}, TP_{scaled-R}, t, \Delta t_{adaptive}\} \leftarrow SystemScaler (TP_{DS-R}, f_o, f, n_{iter}, e_p, \Delta t_{adaptive}, coor_{obs}, t, A, B, C, DS_{index}, coor_{boundary}, v)$
- 8 $T_p \leftarrow TP_{scaled-R} \cup T_p$
- 9 Count the number of new and repeated cells visited in environment
- 10 Calculate tc and t
- 11 $tc_{new} \leftarrow tc$
- 12 **if** ($tc < dc$) **then**
- 13 | Stop;
- 14 **end**
- 15 **if** ($\frac{\text{New cells visited in } [t-\Delta t : t]}{\text{Total of new and repetitive cells visited in } [t-\Delta t : t]} \geq c \frac{\text{Total unvisited cells in } [0 : t-\Delta t]}{\text{Total number of cells}}$) **then**
- 16 **if** ($tc_{new} == tc_{old}$) **then**
- 17 | $DS_{index} \leftarrow DS_{index} + 1$
- 18 **end**
- 19 $TP_{scaled-R}(1, :) \leftarrow TP_{scaled-R}(n_{TP_{DS-R}}, :)$
- 20 $TP_{DS-R}(1, :) \leftarrow TP_{DS-R}(n_{TP_{DS-R}}, :)$
- 21 Total unvisited cells \leftarrow Total unvisited cells — new cells visited
- 22 **else**
- 23 $\{TP_{DS-R}, TP_{scaled-R}, t, T_p, tc\} \leftarrow MapZoning (TP_{DS-R}, TP_{DS-R-logistic}, TP_{scaled-R}, f_o, f, T_p, coor_{obs}, \Delta t_{constant}, t, r, coor_{boundary}, \Delta n_h, t_h, dc, tc, v)$
- 24 **end**
- 25 **end**

3.1 Orientation Control

To avoid repetitive coverage, we keep track of the coverage rate in the previous iteration (tc_{old}) and the current iteration (tc_{new}). Each Arnold system coordinate is associated with an index number (DS_{index}), with index numbers 1, 2, and 3 representing coordinates $x(t)$, $y(t)$, and $z(t)$, respectively. At the start of the coverage task, an initial index number (DS_{index}) is selected to be mapped into robot's kinematic equations. During the coverage task, line 6 of Algorithm 1 assigns the coverage rate obtained in previous iteration to tc_{old} and line 11 sets the coverage rate calculated in the current iteration (tc) to tc_{new} .

If there is no change identified in the coverage rate, i.e., tc_{new} is equal to tc_{old} , the robot steers to cover new cells in neighboring regions by switching the index number (DS_{index}). Lines 19 and 20 of Algorithm 1 will then define the robot and DS initial conditions by replacing the first entries of the temporary matrixes $TP_{scaled-R}$ and TP_{DS-R} by their current last entries (denoted by the row index, $n_{TP_{DS-R}}$). The matrixes $TP_{scaled-R}$ and TP_{DS-R} contain the scaled and unscaled robot's coordinates of the Arnold system generated by *SystemScaler* function, respectively. The algorithm then updates the number of unvisited cells in line 21 in order to calculate the criterion relation in line 15 in the next iteration. The performance can be further improved using a second technique called map zoning, as discussed in Section 3.2.

3.2 Map Zoning

To further scan for new cells and increase dispersion of the robot's path, the robot uses a map zoning method that breaks the map down into 16 individual zones and generates a priority list (I_{zone}) containing: each zone's midpoint, the distance (d) between the robot's current position and the midpoint coordinates of each zone, the robot's current zone and position, and the coverage density (ρ) of each zone. For a robot traversing an environment without obstacles, the algorithm prioritizes density over distance for selecting the best zone for coverage. For map zoning in environments with obstacles, distance is prioritized over density to select

Algorithm 2: *MapZoning* (TP_{DS-R} , $TP_{DS-R-logistic}$, $TP_{scaled-R}$, f_o, f, T_p , $coord_{obs}$, $\Delta t_{constant}$, t, r , $coord_{boundary}$, $n_h, \Delta n_h, t_h, dc, tc, v$)

```

Inputs:  $TP_{DS-R}$ ,  $TP_{DS-R-logistic}$ ,  $TP_{scaled-R}$ ,  $f_o, f, T_p$ ,  $coord_{obs}$ ,  $\Delta t_{constant}$ ,  $t, r$ ,  $coord_{boundary}$ ,  $n_h, \Delta n_h, t_h, dc, tc, v$ 
Outputs:  $TP_{DS-R}$ ,  $TP_{scaled-R}$ ,  $t, T_p, tc$ 
 $TP_{DS-R-logistic}(1, 2:3) \leftarrow TP_{scaled-R}(n_{TP_{DS-R}})$ 
while ( $tc < dc$ ) do
3   Generate the list  $l_{zone}$ 
4   while ( $l_{zone} \neq \emptyset$ ) do
5     Find the zone in  $l_{zone}$  associated with least distance  $d_{min}$ 
6     if (multiple zones associate with  $d_{min}$ ) then
7       |  $[X_{end}, Y_{end}] \leftarrow$  midpoint coordinates associated with  $\rho_{min}$  and  $d_{min}$ 
8     else
9       |  $[X_{end}, Y_{end}] \leftarrow$  midpoint coordinates associated with  $d_{min}$ 
10    end
11     $t_{TR} \leftarrow [0: \Delta t_{constant} : d_{min}/v]$ 
12     $TP_{DS-R-logistic} \leftarrow$  Eqs. (2) and (4)
13    if ( $TP_{DS-R-logistic}(:, 2:3) == \infty$  or NaN) then
14      Stop;
15    end
16    Generate matrix  $[\hat{X}, \hat{Y}]$ 
17    for ( $i = 1, 2, \dots, m$ ) do
18      |  $[X'(i, 1), Y'(i, 1)] \leftarrow$  Eq. (6)
19      | if ( $[X'(i, 1), Y'(i, 1)]$  is outside or close to a boundary) then
20        | |  $[X'(i, 1), Y'(i, 1)] \leftarrow$  Eq. (7)
21      | end
22      | if ( $[X'(i, 1), Y'(i, 1)]$  is outside a boundary) then
23        | | Stop;
24      | end
25    end
26     $\{[X', Y'], t, n_h\} \leftarrow$  LogisticObstacleAvoid ( $[X', Y'], [\hat{X}, \hat{Y}], TP_{DS-R-logistic}, [X_{end}, Y_{end}], t, \Delta t_{constant}, coord_{obs}, f_o, t_h, m$ )
27     $T_p \leftarrow [X', Y'] \cup T_p$ 
28    Count the number of new and repeated cells visited
29    Calculate  $tc$  and  $t$ 
30     $TP_{scaled-R}(1, :) \leftarrow [X'(n_{map}, 1), Y'(n_{map}, 1)]$ 
31     $TP_{DS-R}(1, :) \leftarrow [TP_{DS-R}(n_{TP_{DS-R}}, 1:3), X'(n_{map}, 1)/f, Y'(n_{map}, 1)/f]$ 
32    if ( $[X'(n_{map}, 1), Y'(n_{map}, 1)] == [X_{end}, Y_{end}]$  or  $tc > dc$ ) then
33      | Break;
34    end
35    if ( $n_h == t_h$ ) then
36      |  $TP_{DS-R-logistic}(2: n_{TP_{DS-R-logistic}}, :) \leftarrow \emptyset$ 
37      |  $TP_{DS-R-logistic}(1, 2:3) \leftarrow [X'(n_{map}, 1), Y'(n_{map}, 1)]$ 
38      | Eliminate the zone that the robot failed to reach from  $l_{zone}$ 
39      | if ( $l_{zone} == \emptyset$ ) then
40        | |  $t_h \leftarrow t_h + \Delta n_h$ 
41      | end
42    end
43  end
44  if ( $l_{zone} == \emptyset$ ) then
45    | Continue;
46  end
47  if ( $[X'(n_{map}, 1), Y'(n_{map}, 1)] == [X_{end}, Y_{end}]$  or  $tc > dc$ ) then
48    | Break;
49  end
50 end

```

the new zone for coverage. The algorithm will then construct a collision-free path to direct the robot from the current position to the new starting point (midpoint). If the robot cannot reach the midpoint of the new zone within a certain number of attempts (t_h), it will perceive that zone as being inaccessible at the time. In this case, Algorithm 2 will remove the entries of the selected new zone from the priority list (l_{zone}) in line 38 and will identify another zone for the robot to scan (lines 5-10 of Algorithm 2). Lines 5-42 of Algorithm 2 repeat these tasks to find a collision-free path to another zone, as long as the priority list (l_{zone})

is not empty. In case the priority list (l_{zone}) becomes empty before finding a collision free path (as verified in lines 44-46), the algorithm generates a new priority list based on the current position of the robot in line 3, increases the maximum number of attempts (t_h) to avoid an obstacle (in lines 39-41) by Δn_h , and repeats the tasks in lines 5-42 to find a path. In this work, we considered Δn_h as 5 for all tested environments; using a larger number will increase the coverage time.

Algorithm 2 stops executing either if the robot reaches the desired zone, or if the desired coverage rate (dc) is achieved (lines 2, 32-34, 47-49). The second condition might be met even in situations where the robot has not yet reached the desired zone; this happens when the robot covers sufficient number of new cells in its attempts to travel to the new zone. Section 3.2.1 will discuss how Algorithm 2 uses the Logistic map system to generate a direct chaotic and collision free path for the robot to travel to midpoint of the new zone.

3.2.1 Logistic Map Trajectory

In the map zoning technique, the robot uses the Logistic map system to travel chaotically from its current position to the new starting point. To ensure that the robot navigates to the specified zone, Eq. (6) maps the Logistic map robot's trajectory (obtained from Eq. (4)) onto a direct path connecting the current position and the new starting point and verifies if there is a safe distance between the mapped points and the environment boundaries and obstacles (lines 11-26).

Each time Algorithm 1 calls the *MapZoning* function, it passes the matrix $TP_{DS-R-logistic}$ which only includes the DS initial conditions and later on the matrix populates new entries of DS and robot coordinates (in line 12 of Algorithm 2). The robot's initial coordinates (on the path between the two zones) are equal to the last position coordinates of the robot in the current zone (i.e., last point of the previous Arnold trajectory), as defined in line 1 of Algorithm 2.

To determine the number of trajectory points required to travel between the two specified points, line 11 constructs a time vector (t_{TR}) with a constant step size of 0.1s ($\Delta t_{constant}$) and length m . The vector starts from 0 and ends at d_{min}/v , where d_{min}/v is the time taken by the robot to travel from the current position to the new starting point using a straight path. Knowing the length of this time vector, line 12 deploys Eqs. (2) and (4) to generate m new DS and robot position coordinates and assigns those to matrix $TP_{DS-R-logistic}$: the generated robot trajectory points are referred here as matrix $([X, Y])$. If any of the Logistic map trajectory points approach infinity or becomes NaN (not a number), Algorithm 2 terminates with an error. This might happen due to choosing non-chaotic DS initial conditions for the Logistic map system at the beginning of the simulation. Otherwise, line 16 of Algorithm 2 generates m evenly spaced relative trajectory points to map the robot's trajectory points onto a direct chaotic path between two points. The start point of the relative trajectory matrix is the difference between the first point of the Logistic map trajectory and the robot's current position, and the end point is the difference between the last point of Logistic map trajectory and the midpoint of the new zone (i.e., $[X_{end}, Y_{end}]$). Using the Logistic map $([X, Y])$ and the relative trajectory points $([\hat{X}, \hat{Y}])$, Algorithm 2 generates m mapped trajectory points, while repeating the lines 18-24. Line 18 uses Eq. (6) to generate the mapped trajectory points $([X', Y'])$:

$$\begin{aligned} X' &= X + \hat{X} \\ Y' &= Y + \hat{Y} \end{aligned} \tag{6}$$

If any points are located outside the environment boundaries or is closer than a certain distance to any boundary, line 20 of Algorithm 2 uses Eq. (7) to translate the mapped trajectory point to a safe distance from the boundary to avoid collision. Section 4 explains Eq. (7) and the boundary avoidance method. Improper choices of the DS initial conditions for the Logistic map system might also cause generation of a mapped point far away from the boundary, in which case the simulation will terminate. Otherwise, the function *LogisticObstacleAvoid* (or Algorithm 4), will construct a new path from the previous valid mapped point to avoid the obstacle.

In case the robot reaches the midpoint of the new zone, it should be prepared to start coverage of the new zone using the Arnold system in the next iteration (line 7 of Algorithm 1). Therefore, line 30 of Algorithm 2

assigns the last mapped trajectory points in matrix $[X', Y']$ as the robot's ICs to first entry of matrix $TP_{scaled-R}$, and line 31 assigns the last DS coordinates of the Arnold system and unscaled mapped points to first entry of matrix TP_{DS-R} . Otherwise, if the algorithm determines (in line 35) that the robot has reached the maximum number of attempts to avoid the obstacle, it will remove all the entries of matrix $TP_{DS-R-logistic}$ except the Logistic map DS initial conditions in line 36. It will then define the last mapped trajectory point in matrix $[X', Y']$ as the robot's current position in line 37.

3.3 System Scaling

In the system scaling technique, a scaling factor (f) is applied to scale the robot's trajectories, allowing it to adjust the coverage density based on the robot's sensing range and to vary the coverage extent based on the environment size. To determine the influence of the scaling technique on the robot's trajectory, the Arnold system with three different scaling factor (0.1, 1 and 2) was used to cover the same environment in the same period of 2.16×10^3 seconds. The robot has a sensing range of 1 m in this example. Fig. 3 depicts the results which show the strong influence of scaling factor on the trajectories extent and coverage density. As observed in Figs. 3 (a)-(c), the robot manages to cover 18%, 40%, and 54% of the map with the scaling factor of 0.1, 1, and 2, respectively. In this specific example, the increase in the scaling factor and therefore the coverage extent has sped up the coverage task. Section 5 describes the results associated with additional system scaling tests.

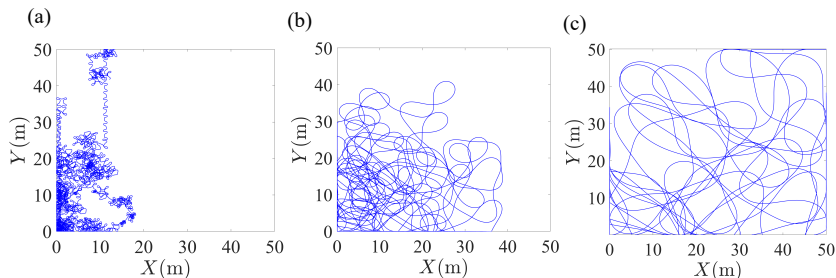


Fig. 3. Robot's trajectory created using the Arnold system with: (a) $f = 0.1$, (b) $f = 1$, (c) $f = 2$.

Algorithm 3 generates and returns the robot's trajectory using the Arnold system. In line 1, Algorithm 3 scales the robot's current position coordinates in matrix TP_{DS-R} using the scaling factor f and assigns the results to the first row of the matrix $TP_{scaled-R}$, which includes the robot's scaled coordinates. Lines 3-24 will then repeat to generate n new trajectory points. These points create the proposed path for the robot to scan the current region. The algorithm sets the number of iterations (n) to generate 1000 new entries of trajectory points, which was selected via analysis.

To integrate Eqs. (1) and (3) and compute the new DS and robot's coordinates, Algorithm 3 uses a fourth-order Runge- Kutta (RK4) method suggested by [22]. However, instead of a constant time step, the present study proposes to use an adaptive time step ($\Delta t_{adaptive}$); the preliminary study demonstrated that a constant time step causes error in calculation of the robot trajectory points that accumulates over time. The study also showed strong influence of the initial choice of adaptive time step on accuracy of the points and coverage time. The optimal value for initial time step was found to be 0.1 seconds.

To apply the adaptive RK4 method, we compare the difference of the robot coordinates obtained using different time steps, assigning the dynamic and robot trajectory points associated with current time step ($\Delta t_{adaptive}$) to matrix TP_{DS-R} if the output does not exceed the error tolerance (e_p). Lines 11-13 will terminate the simulation if the NaN or infinity trajectory points are observed among the newly generated points (similar to lines 13-15 of Algorithm 2).

Lines 14-19 of Algorithm 3 transfer any trajectory point that lie outside or close to any boundary or obstacle using Eqs. (7) and (8). Then in line 20, all the generated robot trajectory points are scaled using the scaling factor f and the results will be stored in matrix $TP_{scaled-R}$. In line 21, we verify if any of the trajectory

points still lie outside the boundary. Line 24 adds the current time to the time step, multiplying $\Delta t_{adaptive}$ by the scaling factor to maintain a constant velocity for the robot. This is necessary because the distance between the points will change after the scaling.

Algorithm 3: *SystemScaler* ($TP_{DS-R}, f_o, f, n_{iter}, e_p, \Delta t_{adaptive}, coor_{obs}, t, A, B, C, DS_{index}, coor_{boundary}, v$)

Inputs: $TP_{DS-R}, f_o, f, n_{iter}, e_p, \Delta t_{adaptive}, coor_{obs}, t, A, B, C, DS_{index}, coor_{boundary}, v$
Outputs: $TP_{DS-R}, TP_{scaled-R}, t, \Delta t_{adaptive}$

```

1   $TP_{scaled-R}(1, 1:2) = f TP_{DS-R}(1, 4:5)$ 
2  for ( $i = 1, 2, \dots, n$ ) do
3     $[x(t), y(t), z(t), X(t), Y(t)] \leftarrow$  Eqs. (1) and (3)
4     $[x_{half}(t), y_{half}(t), z_{half}(t), X_{half}(t), Y_{half}(t)] \leftarrow$  Eqs. (1) and (3)
5    if ( $|X(t) - X_{half}(t)| > e_p$  or  $|Y(t) - Y_{half}(t)| > e_p$ ) then
6       $TP_{DS-R}(i+1, :) \leftarrow [x_{half}(t), y_{half}(t), z_{half}(t), X_{half}(t), Y_{half}(t)]$ 
7       $\Delta t_{adaptive} \leftarrow \Delta t_{adaptive}/2$ 
8    else
9       $TP_{DS-R}(i+1, :) \leftarrow [x(t), y(t), z(t), X(t), Y(t)]$ 
10   end
11   if ( $TP_{DS-R}(i+1, :) == \infty$  or NaN) then
12     Stop;
13   end
14   if ( $TP_{DS-R}(i+1, 4:5)$  is outside or close to a boundary) then
15      $TP_{DS-R}(i+1, 4:5) \leftarrow$  Eq. (7)
16   end
17   if ( $TP_{DS-R}(i+1, 4:5)$  is inside or close to an obstacle) then
18      $TP_{DS-R}(i+1, 4:5) \leftarrow$  Eq. (8)
19   end
20    $TP_{scaled-R}(i+1, 1:2) = f TP_{DS-R}(i+1, 4:5)$ 
21   if ( $TP_{scaled-R}(i+1, 1:2)$  is outside a boundary) then
22     Stop;
23   end
24    $t \leftarrow t + \Delta t_{adaptive} f$ 
25 end

```

Ultimately, to ensure fast exploration of environments, the unknown obstacles should not interfere with the robot's efforts to cover the environment. The obstacle avoidance strategies established in this study enable the robot to adapt the plan once facing the obstacles, to avoid them smoothly, and resume the task quickly based on the new plan.

4 OBSTACLE AVOIDANCE TECHNIQUES

4.1 Boundary Avoidance

Upon integrating the Arnold or Logistic map system and incorporating Eq. (3) or (4) for mapping, a certain number of the robot's coordinates lied very close to the map boundaries or outside them. Eq. (7) adapts a mirror-mapping technique (suggested by [22]) to translate the robot's X or Y coordinates that lied close to the boundaries or outside the map using coordinate transformation:

$$\begin{aligned} X &= -X + 2(M_{left} \pm f_o) \\ Y &= -Y + 2(N_{upper} \pm f_o) \end{aligned} \quad (7)$$

where M and N represent the column and row coordinates, respectively; *left* and *upper* refer to left and upper boundary, respectively; and f_o is a factor that determines how far the mirrored points offset into the map with respect to the boundaries. The value of f_o is chosen based on the robot's size and characteristics of its sensor, such as range and the reference point. This study considered 0.5 meters as a safe distance from the boundaries.

Eq. (7) changes its variables based on the trajectory point's location with respect to the boundaries. For instance, if the X -coordinate of the point was positioned outside or close to the left boundary, then Eq. (7) will shift only the X -component of the point and the Y -component will remain unchanged. If the X -coordinate was positioned outside or close to the right boundary, then M_{left} is substituted by M_{right} to translate the X -

component. A similar procedure would take place if the Y -component lied outside or close to the boundaries. If both coordinates lied outside or near a boundary, then both components would be translated, depending on the position of the coordinates with respect to the boundaries. The sign before f_o will change as well depending on the trajectory point's location with respect to the boundaries. A '-' sign before f_o will appear when the points lie outside or close to the right/upper boundaries. A '+' sign will take place when the points lie outside or close to the left/lower boundaries. By incorporating this technique of mirror mapping, the robot was confined within the boundaries for its coverage task. Section 4.2 establishes techniques to avoid obstacles throughout the environment.

4.2 Obstacle Avoidance

The robot uses different obstacle avoidance techniques depending on whether the Arnold or the Logistic map system is employed for navigation. Section 4.2.1 and 4.2.2 will discuss these techniques.

4.2.1 Obstacle Avoidance for Arnold System

The obstacle avoidance designed for the Arnold system enables the robot to sense the boundaries of the obstacles and if the generated trajectory point is inside the obstacle or very close to it. Eq. (7) presented in previous section for boundary avoidance, could be also used for obstacle avoidance. However, Eq. (7) might place the mirror-mapped points much further away from the obstacle and the current robot's position. As a result, with a small time step, the robot should increase its velocity to travel from the current position to the mirror-mapped point and this violates the constant robot's velocity assumption made by this study. Therefore, this study established Eq. (8) to position the robot away from the obstacle using the offset factor f_o (lines 17-19 of Algorithm 3), while maintaining a constant velocity for the robot:

$$\begin{aligned} X &= M_{left} \pm f_o \\ Y &= N_{upper} \pm f_o \end{aligned} \tag{8}$$

Eq. (8) resembles Eq. (7); the same representation is used for the variables. Similar to Eq. (7), the row and column coordinates and sign before the offset factor (f_o) change depending on where the trajectory point is located with respect to the obstacle. The trajectory point position is also the deciding factor on which relation in Eq. (8) to use to transfer the point. Using this technique, the algorithm always ensures that the trajectory points do not fall inside the obstacles and the robot stays away from the obstacles.

When using trajectories generated by the Arnold system, the above-mentioned technique enabled the robot to avoid the obstacles impeccably. The Logistic map system uses Eq. (8) for mapping as well; however, it was not as straightforward to avoid obstacles when using the Logistic map system trajectories. Section 4.2.2 develops a new obstacle avoidance technique for Logistic map-based navigation.

4.2.2 Obstacle Avoidance for Logistic map system

In an environment with unknown obstacles, the robot might face two challenges when it uses the Logistic map system to travel to midpoint of a new zone: (1) the midpoint might be located in a zone surrounded by an unknown obstacle or (2) the path generated by the Logistic map system might pass through an obstacle. With no rigorous obstacle avoidance technique in place, the robot might spend considerable time on finding a way to reach the target midpoint or fall into a never-ending cycle as trying to travel to an out-of-reach midpoint. To prevent these issues, a new method was established to avoid obstacles when traveling between two points in online coverage problems. Line 26 of Algorithm 2 invokes Algorithm 4 to find an obstacle free path for the robot to travel to midpoint of a new zone, if possible.

Fig. 4 illustrates the technique used to find such path. In this figure, the midpoint of new zone (goal) is located inside an obstacle. At the beginning, the algorithm constructs a path to reach the goal from robot's initial point (or current position). The robot travels on this path until it detects the obstacle and realizes that the next point is inside the obstacle. The algorithm uses the mirror-mapping technique (Eq. (8)) to transfer

the detected point away from the obstacle. The algorithm considers this as the first attempt ($n_h = 1$) to travel to midpoint of the new zone. The algorithm will then construct a new path from the mirror-mapped point to the goal. The variable n_h increments by one, each time the attempt to reach the goal is not successful, i.e., the constructed path passes through the obstacle. The procedure to find an obstacle free path is repeated until the robot reaches the goal (i.e., an obstacle free path is found) or the number of attempts (n_h) reaches the maximum number of attempts (t_h). In case of latter, the robot realizes that it is either impossible or very time-consuming to travel to the target zone; therefore, it finds the next best zone to land using Algorithm 2 (as discussed in section 3.2.1).

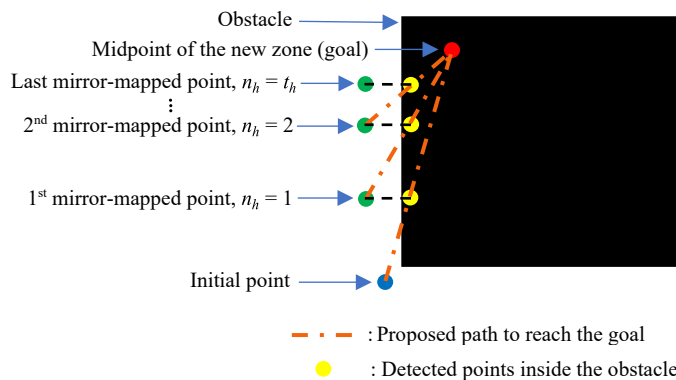


Fig 4. A schematic of the obstacle avoidance technique using Logistic map.

Algorithm 2 (lines 11-25) constructs the first proposed path from the robot's current position to the midpoint of new zone and then in line 26 calls Algorithm 4 to verify if the path is obstacle free. Algorithm 4 follows the steps shown in Fig. 4 to examine the path and to construct a new path, if necessary. In lines 2-5 of Algorithm 4, if the next trajectory point lies within any detected nearby obstacle, it will transfer the point away from the obstacle using the mirror-mapping technique (Eq. (8)), discarding unreachable points. The algorithm follows a similar procedure to what described in Section 3.2.1 to construct the new mapped trajectory. Each new trajectory will be shorter than the previous ones (i.e., less number of points is required), because in each attempt the robot becomes closer to the goal point, as shown in the paths constructed for $n_h \geq 1$ in Fig. 4. To update the required number of points (m), line 6 of Algorithm 4 subtracts from m , the number of points that the robot has already traversed on previous trajectories toward goal. Then in line 7, Algorithm 4 generates m evenly spaced relative trajectory points. In line 8, the algorithm sets the number of attempts (n_h) equal to one, which indicates the first-time obstruction of the robot's path by an obstacle. Lines 10-25 of Algorithm 4 repeat to generate an obstacle free path until n_h becomes equal to t_h or the robot reaches the midpoint of the new zone (goal). Line 9 will verify the former condition and lines 23-25 will examine the latter. If either condition is satisfied, Algorithm 4 stops executing (lines 27 and 24) and returns the valid trajectory points, time, and n_h .

For a $50 \text{ m} \times 50 \text{ m}$ environment, the maximum number of attempts (t_h) is initially set to 10, at the start of the coverage task. For environment sizes of $100 \text{ m} \times 100 \text{ m}$ and $200 \text{ m} \times 200 \text{ m}$, a higher initial t_h value is considered. As the obstacles size increase in larger environments, the robot should make more attempts to avoid them. These initial t_h values allowed the robot to reach the desired zone with reasonable efforts and at the same time prevented an increase in the coverage time.

With the chaos control and obstacle avoidance techniques induced into the chaotic path planning algorithm, the robot was able to visit all regions in the map, avoid boundaries and obstacles, and cover 90% of the map in a short time. The next Section will discuss the robot's trajectory and the coverage time in environments with and without obstacles.

Algorithm 4: *LogisticObstacleAvoid* ($[X', Y']$, $[\hat{X}, \hat{Y}]$, $TP_{DS-R-logistic}$, $[X_{end}, Y_{end}]$, t , $\Delta t_{constant}$, $coor_{obs}$, f_o , t_h , m)

Inputs: $[X', Y']$, $[\hat{X}, \hat{Y}]$, $TP_{DS-R-logistic}$, $[X_{end}, Y_{end}]$, t , $\Delta t_{constant}$, $coor_{obs}$, f_o , t_h , m
Outputs: $[X', Y']$, t , n_h

```

1  for ( $i = 1, 2, \dots, m$ ) do
2      if ( $[X'(i,1), Y'(i,1)]$  is inside an obstacle) then
3           $[X'(i+1:m, 1), Y'(i+1:m, 1)] \leftarrow \emptyset$ 
4           $[\hat{X}, \hat{Y}] \leftarrow \emptyset$ 
5           $[X'(i, 1), Y'(i, 1)] \leftarrow \text{Eq. (8)}$ 
6           $m \leftarrow m - i + 1$ 
7          Generate matrix  $[\hat{X}, \hat{Y}]$  using  $TP_{DS-R-logistic}(i: n_{TP_{DS-R-logistic}}, 2:3)$ 
8           $n_h \leftarrow 1$ 
9          while ( $n_h < t_h$ ) do
10             for ( $i = i, i+1, \dots, n_{TP_{DS-R-logistic}}$ ) do
11                  $[X'(i,1), Y'(i,1)] \leftarrow \text{Eq. (6)}$ 
12                 if ( $[X'(i,1), Y'(i,1)]$  is inside an obstacle) then
13                      $[\hat{X}, \hat{Y}] \leftarrow \emptyset$ 
14                      $[X'(i, 1), Y'(i, 1)] \leftarrow \text{Eq. (8)}$ 
15                      $m \leftarrow m - i + 1$ 
16                     Generate matrix  $[\hat{X}, \hat{Y}]$  using  $TP_{DS-R-logistic}(i: n_{TP_{DS-R-logistic}}, 2:3)$ 
17                      $n_h \leftarrow n_h + 1$ 
18                     Break
19                 else
20                      $t \leftarrow t + \Delta t_{constant}$ 
21                 end
22             end
23             if ( $i == n_{TP_{DS-R-logistic}}$ ) then
24                 Break
25             end
26         end
27         Break
28     else
29          $t \leftarrow t + \Delta t_{constant}$ 
30     end
31 end

```

5 RESULTS

This section compares the performance of systems with different chaos control methods against the original Arnold system in unknown environments with different obstacle configurations and sizes. Table 1 compares the performance of the Arnold system before and after employing a single or a combination of chaos control techniques, while varying the environment size, robot's sensing range (SR), and number of obstacles (N_{obs}). The values of the coverage criterion factor (c), the initial index number (DS_{index}), and the scaling factor (f) were selected to achieve the minimum coverage time for the systems. The initial index number specifies the DS coordinate used for mapping the chaotic behavior into the robot's controller (see Eq. (3)) at the start of the coverage task. The orientation control technique might change this number in the next iterations, if there is no increase in the total coverage rate (lines 16-18 of Algorithm 1). Nevertheless, the initial value selected for DS_{index} is critical as it can significantly change the path planner's performance and influence the coverage time. The coverage criterion factor c (associated with map zoning technique) is a value between 0 to 1; it determines the conditions under which the robot should leave the current zone and travel to a new zone to improve the coverage uniformity and reduce the coverage time. Finally, the scaling factor f is used to adjust the trajectories extent and density based on the sensing range and the environment size.

To determine the optimal value of c , initial index number, and scaling factor f for each of the cases presented in Table 1, the trial and error tests were conducted. In these tests, the parameter c was varied between 0.1 and 1, the initial index number was varied between the integers $[1..3]$, and the factor f was changed in the range between 1 and 6. The c values below 0.1 were not considered in these tests as those

values would not provide enough time for the robot to properly explore the current zone. For factor f , the initial tests indicated that the values over 6 or under 1 are not effective and result in a significant increase in the coverage time in the examined environments, therefore those values were abandoned in the future tests. The conducted tests provided the best values for parameters c , initial index, and f for each method and environment; Table 1 uses these values to compare the performance of different methods. Table 1 also incorporates the results of coverage using the Logistic map system (case 11) to demonstrate superior performance of the Arnold system in covering the areas.

Table 1: Performance of different systems in various unknown environments.

System type	No.	Space size	SR (m)	f	N_{obs}	c	Initial DS_{index}	CT	% (hours) improv. w.r.t original Arnold	PR
Original Arnold	1	50m × 50m	1	N/A	0	N/A	3	6.95×10^3	N/A	2.6
	2	50m × 50m	1	N/A	1	N/A	3	6.60×10^3	N/A	N/A
	3	50m × 50m	1	N/A	4	N/A	3	6.05×10^3	N/A	N/A
	4	50m × 50m	1	N/A	5	N/A	2	1.04×10^4	N/A	N/A
	5	100m × 100m	1	N/A	0	N/A	3	3.24×10^4	N/A	3
	6	100m × 100m	1	N/A	5	N/A	3	2.77×10^4	N/A	N/A
	7	200m × 200m	1	N/A	0	N/A	3	1.72×10^5	N/A	3.9
	8	200m × 200m	1	N/A	5	N/A	3	9.92×10^4	N/A	N/A
	9	200m × 200m	4	N/A	0	N/A	3	5.36×10^4	N/A	5.7
	10	200m × 200m	4	N/A	5	N/A	3	3.51×10^4	N/A	N/A
Logistic map	11	50m × 50m	1	N/A	0	N/A	N/A	2.34×10^4	-236.7 (~ 4.57 hrs↑)	8.7
Arnold with 1st chaos control technique	12	50m × 50m	1	N/A	0	N/A	3	6.40×10^3	7.9 (~ 0.15 hrs↓)	2.4
	13	50m × 50m	1	N/A	1	N/A	3	5.45×10^3	17.4 (~ 0.32 hrs↓)	N/A
	14	50m × 50m	1	N/A	4	N/A	2	6.50×10^3	-7.4 (~ 0.13 hrs↑)	N/A
	15	50m × 50m	1	N/A	5	N/A	3	7.40×10^3	28.8 (~ 0.83 hrs↓)	N/A
	16	100m × 100m	1	N/A	0	N/A	3	3.89×10^4	-20.1 (~ 1.81 hrs↑)	3.6
	17	100m × 100m	1	N/A	5	N/A	3	2.13×10^4	23.1 (~ 1.78 hrs↓)	N/A
	18	200m × 200m	1	N/A	0	N/A	3	1.48×10^5	14.0 (~ 6.67 hrs↓)	3.4
	19	200m × 200m	1	N/A	5	N/A	3	8.35×10^4	15.8 (~ 4.36 hrs↓)	N/A
Arnold with 3rd chaos control technique	20	200m × 200m	1	1.90	0	N/A	3	1.13×10^5	34.3 (~16.39 hrs↓)	2.6
	21	200m × 200m	1	1.30	5	N/A	3	8.33×10^4	16.0 (~ 4.41 hrs↓)	N/A
	22	200m × 200m	4	3.35	0	N/A	3	2.59×10^4	51.8 (~ 7.69 hrs↓)	2.7
	23	200m × 200m	4	1.76	5	N/A	3	1.79×10^4	49.0 (~ 4.78 hrs↓)	N/A
Arnold with 1st and 2nd chaos control techniques (Arnold-Logistic)	24	50m × 50m	1	N/A	0	1.0	1	4.70×10^3	32.4 (~ 0.63 hrs↓)	1.7
	25	50m × 50m	1	N/A	1	0.85	3	5.20×10^3	21.2 (~ 0.39 hrs↓)	N/A
	26	50m × 50m	1	N/A	4	0.15	3	6.03×10^3	0.3 (~ 0.01 hrs↓)	N/A
	27	50m × 50m	1	N/A	5	0.80	1	4.35×10^3	58.2 (~ 1.68 hrs↓)	N/A
	28	200m × 200m	1	N/A	0	0.10	3	8.93×10^4	48.1 (~ 22.97 hrs↓)	2.1
	29	200m × 200m	1	N/A	5	0.10	3	9.58×10^4	3.4 (~ 0.94 hrs↓)	N/A
	30	200m × 200m	4	N/A	0	0.10	3	2.28×10^4	57.4 (~ 8.56 hrs↓)	2.4
	31	200m × 200m	4	N/A	5	0.10	3	1.96×10^4	44.1 (~ 4.31 hrs↓)	N/A
Arnold with all three chaos control techniques	32	200m × 200m	1	1.64	0	0.10	3	9.07×10^4	47.3 (~22.58 hrs↓)	2.1
	33	200m × 200m	1	1.50	5	0.10	3	6.45×10^4	35 (~ 9.64 hrs↓)	N/A
	34	200m × 200m	4	1.25	0	0.10	3	2.08×10^4	61.2 (~9.11 hrs↓)	2.2
	35	200m × 200m	4	1.80	5	0.10	3	1.63×10^4	53.6 (~ 5.22 hrs↓)	N/A

In obstacle-free environments, Table 1 compares the coverage time of the Arnold-based systems as well with that of an optimal path planner (T_{Opt}) using the performance ratio $PR (= CT/T_{Opt})$. The optimal path planner uses back and forth motions to cover the space (see Fig. 5). Sections 5.1 and 5.2 discuss the results in small environments (50m×50m) and large environments (100m×100m and 200m×200m), respectively.

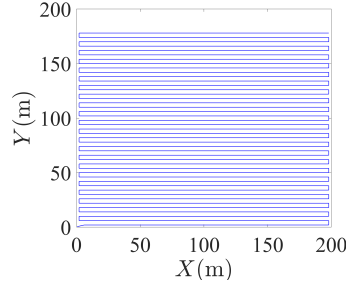


Fig 5. Robot's optimal trajectories (SR=4 m) for 90% coverage of the space.

5.1 Coverage Results in Small Environments

This section discusses the coverage results of the original Arnold system, the Arnold system with first chaos control technique, and the Arnold-Logistic system in a $50\text{ m} \times 50\text{ m}$ environment with and without obstacles, as depicted in Fig. 6. In all these cases, the robot could successfully cover 90% of the environment and simultaneously avoid obstacles in its path. Figs. 6(a)-(d) show the robot's trajectories generated using

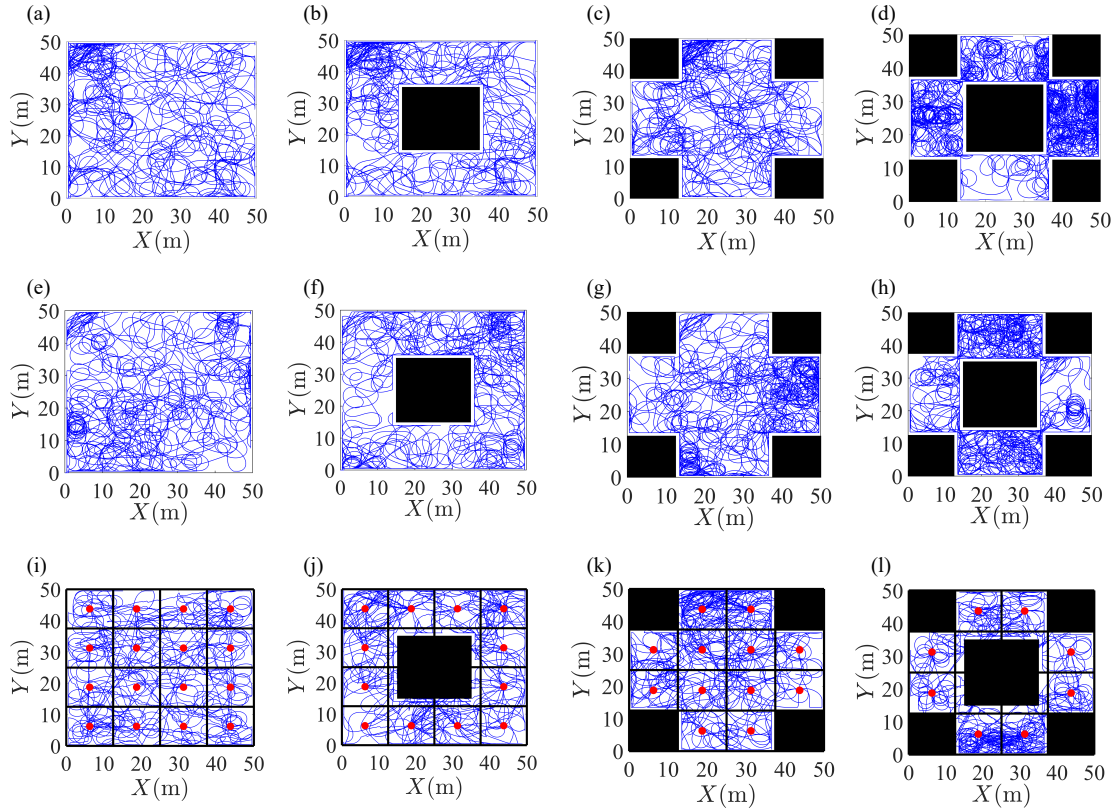


Fig 6. Robot's trajectory for: (a-d) Original Arnold (SR=1 m), (e-h), Arnold with 1st chaos control technique (SR=1 m), and (i-l) Arnold-Logistic system (SR=1 m). Dot: zone's midpoint; Black square: obstacle.

the original Arnold system; dense trajectories can be observed in some parts of the environment specially in the case of the environment with five obstacles. Using the first chaos control technique in Figs. 6(e)-(h) has mitigated this issue in all $50\text{ m} \times 50\text{ m}$ environments except for the environment with four obstacles (Fig.6(g)). The results in Table 1 agree with this observation. Based on Table 1, the first control technique has decreased the coverage time in most scenarios, however in two cases (including the case shown in Fig. 6(g)), it has degraded the performance. This is because in certain iterations, the DS keeps generating

trajectories that can mostly extend to adjacent regions and change in the index number (DS_{index}) could not help the robot to extend them quickly to more distant areas.

Adding the second control technique can help to overcome this issue and guide the robot to navigate to other distant regions. Figs. 6(i)-(l) and Table 1 show the effectiveness of the map zoning technique in decreasing the repetitive coverage and increasing the coverage uniformity in all $50\text{ m} \times 50\text{ m}$ environments, the exception has been the configuration with four obstacles (case 26) where the improvement has not been significant. The greatest improvement corresponds to configuration with five obstacles (case 27) where using the Arnold-Logistic system has led to %58.2 reduction in coverage time ($\sim 1.68\text{ hrs}$ ↓) compared to the original Arnold system. As indicated by the performance ratio (PR), the Arnold-Logistic planner's performance is fairly close to optimal in small obstacle-free spaces.

5.2 Coverage Results in Large Environments

We show that system scaling improves performance by adjusting the system trajectories based on the sensing range and the environment size. Table 1 presents the results of the Arnold system performance after adding the system scaling technique in a $200\text{ m} \times 200\text{ m}$ environment with zero and five obstacles and using a robot with 1 m and 4 m sensing range. Using the system scaling technique has significantly improved the performance in all cases. Comparing the results with those of Arnold-Logistic system, one observes very close performance in configurations in which the robot has 4 m sensing range. In the environment with five obstacles and 1 m sensing range, using the Arnold with system scaling technique (case 21) led to significantly more reduction in the coverage time. The opposite holds for the environment without obstacle and 1 m sensing range (case 20 versus case 28). Overall, the Arnold with system scaling technique presented a remarkably good performance, considering that it corresponds to a much less complex algorithm. Therefore, in situations where the computational power is limited, it might be preferred to use the Arnold with third technique instead of the Arnold-Logistic or combinations of three methods.

However, in applications where computational power is not a concern and high performance and low coverage time are priority, it would be ideal to use Arnold-Logistic in conjunction with the third control technique. As observed in Table 1, the Arnold with all three chaos control techniques performs better than either Arnold with third technique or Arnold-Logistic systems in all cases except for case 32 where the percentage of improvement is very close to case 28 (which uses Arnold-Logistic approach). Comparing the results of case 33 with those of case 19, 21, and 29 demonstrates the benefit of combining all three techniques, i.e., simultaneous application of all three techniques can realize a high level of performance that could not be otherwise achieved using any single technique.

Evaluating the performance ratio (PR) in large obstacle-free spaces in Table 1 once again confirms the effectiveness of the 3rd technique, Arnold-Logistic technique, and their combinations in closing the gap between the chaotic planners and the optimal system performance.

Figs. 7 and 8 depict the robot trajectories associated with some of the cases presented in Table 1. Fig. 7 compares the robot's trajectories created by the original Arnold system with those generated using Arnold system with all three techniques in an environment with no obstacles; Figs. 7(a)-(b) and (c)-(d) correspond to the robot with 1 m and 4 m sensing range, respectively. In both cases, using all three techniques has significantly reduced the repetitive coverage and improved the uniformity. Similar conclusions can be drawn from the trajectories presented in Fig. 8 which compares the coverage using the original Arnold system, the Arnold system with third control technique, and the Arnold system with all three techniques in an environment with five obstacles. Addition of the system scaling in Fig. 8(b) has improved the coverage uniformity and reduced the repetitive coverage; but using the third technique in conjunction with the Arnold-Logistic technique can result in a remarkable enhancement, as shown in Fig. 8(c).

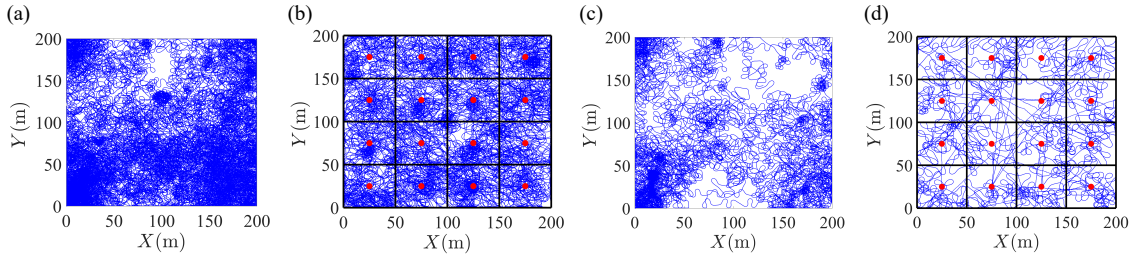


Fig 7. Robot's trajectory in an environment with no obstacle for: (a) Original Arnold (SR=1 m), (b) Arnold with all three chaos control techniques (SR=1 m), (c) Original Arnold (SR=4 m), (d) Arnold with all three chaos control techniques (SR=4 m). Dot: zone's midpoint.

The decision on whether to use the third chaos control technique should be made considering various factors such as the environment estimated size, the estimated density of obstacles in the environment, the properties and coverage density of the generated trajectories by the considered DS, and the robot's sensing capabilities. In terms of parameters associated with each technique (e.g., the scaling factor, the initial index, etc.), their effects on the system performance depend on a wide range of factors and cannot be easily predicted. As a result, finding the best parameters is not often a straightforward task in uncertain environments. Next section will discuss how the parameters influence the performance and the methods that can facilitate estimating the optimal parameters in future studies.

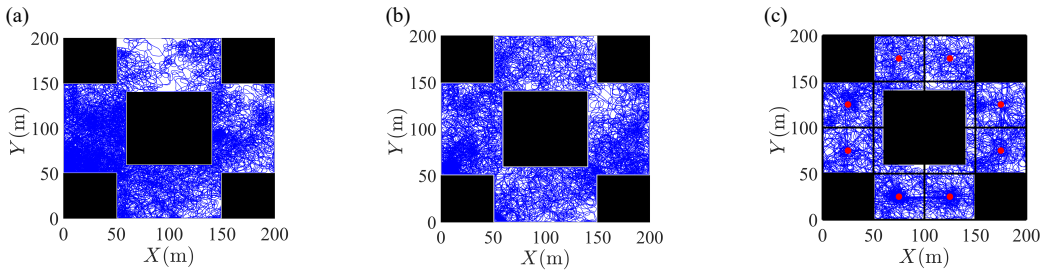


Fig 8. Robot's trajectory in an environment with five obstacles for: (a) Original Arnold (SR=1 m), (b) Arnold with third chaos control technique (SR=1 m), (c) Arnold with all three chaos control techniques (SR=1 m). Dot: zone's midpoint; Black square: obstacle.

5.3 Parameters Influence and Future Directions

Table 1 depicts the optimal parameters for each case, obtained through testing a wide range of parameters. Observing the initial index values, the index value of 3 appears to be the optimal choice for almost all the cases except for a few cases (i.e., cases 4, 14, 24, and 27) where index values 1 or 2 shown to be more effective.

As far as the criterion factor c is concerned, it depends on the size of zones. Since we used the same number of zones for all environments, the size of zones become greater in the larger environments, therefore smaller values of c should suit these environments, as the robot needs to spend more time for exploring larger zones. If a large value of c is selected for such cases, the algorithm would force the robot to travel to the other zones too often and unnecessary traveling might increase the coverage time. On the other hand, for smaller zones, large values of c should be used (e.g., cases 24-27 in Table 1), however, this expectation does not necessarily hold for all the cases in small environments (e.g., cases 24 and 26).

Regarding the scaling factor f , the direct effect of the size of the environment size, level of clutter, and sensing range on the selected scaling factor can be clearly observed in cases where only the third control technique is employed (cases 20-23). In other words, a larger scaling factor is employed in the environments with no obstacle and a robot with high sensing range and for the environments with low clutter and a robot with low sensing range, a smaller scaling factor has been used. However, when the other two control techniques become involved (cases 32-35), there is not always an apparent relationship between the scaling factor and the factors such as the environment size, sensing range, etc. To illustrate, the optimal scaling factor

for case#33 with SR of 1 m and five obstacles is greater than the scaling factor chosen for case#34 where the SR is 4 m and there is no obstacle in the environment.

The reasons behind observing inconsistent values for the three parameters discussed above might be the interdependence of different influencing factors and parameters and the complex relationships they have with one another. The future research should perform a more in-depth study of these effects. Moreover, to deal with uncertainties of the environment and the inherent unpredictability of the chaotic path planner, a deep learning-based decision-making strategy appears to be beneficial as it can help determining the required chaos control techniques and optimizing their associated parameters in each application, based on the initial knowledge about the environment and robot's properties.

This study used a combination of the Arnold and Logistic map system to realize the second chaos control technique and achieve fast coverage, however, future studies can examine combinations of other existing continuous (e.g., Chen, Rucklidge,...) and discrete systems (e.g., Taylor-Chirikov map, Hénon map) for the second control technique that would result in paths with different properties and patterns, suited for different applications.

Lastly, the algorithms in this study were examined on a two-wheeled differential drive robot; different vehicles correspond to different levels of mobility and maneuverability. The future studies should investigate other types of ground robots or UAVs to evaluate the effects of the robot's characteristics on the path planner's performance.

6 CONCLUSIONS

This study proposed new techniques to realize online, fast, and unpredictable search of unknown environments using a mobile robot. Three techniques were established to control the chaotic path planner and enable the robot to automatically cover the environment and adapt to new environments with different sizes and/or obstacle configurations. The third chaos control technique (known as system scaling) provides scalability to the method and allows the robot to adjust the coverage density and extent based on the robots' sensing range and environment size. The study incorporated a new obstacle avoidance technique which allowed the robot to adapt the coverage plan and trajectories when faced with unknown obstacles, to avoid obstacles efficiently and prevent decline in the performance. Evaluating the performance of the individual control techniques and a combination of them in a range of environments showed significant improvement in the performance (i.e., reduced coverage time) for 84% of the tested scenarios. In 8% of cases, negligible improvement in performance was observed and only 8% of cases (associated with the first control technique) exhibited decline in the performance. Combining all three techniques resulted in 49% boost, on average, in performance of the examined cases. Besides providing unpredictability in the agent's motion and thus enabling it to avoid attacks in adversarial environments, the proposed techniques will ensure a level of performance comparable to that of the optimal path planners. Proper selection of the system's parameters is paramount in ensuring the efficient coverage of the environment. Future studies should develop deep learning-based optimization methods to estimate the parameters of the resulting path planning system based on the known properties of the environment and the robot.

ACKNOWLEDGEMENTS

The work was sponsored by the Air Force under MOU FA8750-15-3-6000. The U.S. Government is authorized to reproduce and distribute copies for Governmental purposes notwithstanding any copyright or other restrictive legends. The views and conclusions contained herein are those of the authors and should not be interpreted as necessarily representing the official policies or endorsements, either expressed or implied, of the Air Force or the U.S. Government.

REFERENCES

- [1] J.H. Lee, J.S. Choi, B.H. Lee, K.W. Lee, Complete Coverage Path Planning for Cleaning Task using Multiple Robots, in: Proceedings of the 2009 IEEE International Conference on Systems, Man, and Cybernetics, IEEE, San Antonio, TX, USA, 2009, pp. 3618-3622.
- [2] W. Wang, L. He, Q. Jiang, P.Z. Yikai Shi, Path Planning Algorithm of a Novel Massage Robot, in: 2016 9th International Congress on Image and Signal Processing, BioMedical Engineering and Informatics, IEEE, 2016, pp. 1670-1674.
- [3] E.U. Acar, H. Choset, Y. Zhang, M. Schervish, Path planning for robotic demining: robust sensor-based coverage of unstructured environments and probabilistic methods, *International Journal of Robotics Research*, 22 (2003) 441-466.
- [4] M. Garzón, J. Valente, J.J. Roldán, L. Cancar, A. Barrientos, J. Del Cerro, A multirobot system for distributed area coverage and signal searching in large outdoor scenarios, *Journal of Field Robotics*, 33 (2016) 1087-1106.
- [5] K. Nagatani, Y. Okada, N. Tokunaga, S. Kiribayashi, K. Yoshida, K. Ohno, E. Takeuchi, S. Tadokoro, H. Akiyama, I. Noda, Multirobot exploration for search and rescue missions: A report on map building in RoboCupRescue 2009, *Journal of Field Robotics*, 28 (2011) 373-387.
- [6] V. Spurný, T. Báča, M. Saska, R. Pěnička, T. Krajník, J. Thomas, D. Thakur, G. Loianno, V. Kumar, Cooperative autonomous search, grasping, and delivering in a treasure hunt scenario by a team of unmanned aerial vehicles, *Journal of Field Robotics*, 36 (2019) 125-148.
- [7] A. Das, M. Diu, N. Mathew, C. Scharfenberger, J. Servos, A. Wong, J.S. Zelek, D.A. Clausi, S.L. Waslander, Mapping, planning, and sample detection strategies for autonomous exploration, *Journal of Field Robotics*, 31 (2014) 75-106.
- [8] G. Hitz, E. Galceran, M.É. Garneau, F. Pomerleau, R. Siegwart, Adaptive continuous-space informative path planning for online environmental monitoring, *Journal of Field Robotics*, 34 (2017) 1427-1449.
- [9] T. Wilson, S.B. Williams, Adaptive path planning for depth-constrained bathymetric mapping with an autonomous surface vessel, *Journal of Field Robotics*, 35 (2018) 345-358.
- [10] A. Barrientos, J. Colorado, J.d. Cerro, A. Martinez, C. Rossi, D. Sanz, J. Valente, Aerial remote sensing in agriculture: A practical approach to area coverage and path planning for fleets of mini aerial robots, *Journal of Field Robotics*, 28 (2011) 667-689.
- [11] J. Jin, L. Tang, Coverage path planning on three-dimensional terrain for arable farming, *Journal of field robotics*, 28 (2011) 424-440.
- [12] T. Oksanen, A. Visala, Coverage path planning algorithms for agricultural field machines, *Journal of field robotics*, 26 (2009) 651-668.
- [13] Z.L. Cao, Y. Huang, E.L. Hall, Region filling operations with random obstacle avoidance for mobile robots, *Journal of Robotic systems*, 5 (1988) 87-102.
- [14] D. Kaljaca, B. Vroegindeweij, E. van Henten, Coverage trajectory planning for a bush trimming robot arm, *Journal of Field Robotics*, 37 (2020) 283-308.
- [15] C. Cariou, Z. Gobor, B. Seiferth, M. Berducat, Mobile robot trajectory planning under kinematic and dynamic constraints for partial and full field coverage, *Journal of Field Robotics*, 34 (2017) 1297-1312.
- [16] Y. Nakamura, A. Sekiguchi, The chaotic mobile robot, in: IEEE TRANSACTIONS ON ROBOTICS AND AUTOMATION, IEEE, 2001, pp. 898-904.
- [17] D.-I. Curiac, C. Volosencu, Chaotic Trajectory Design for Monitoring an Arbitrary Number of Specified Locations Using Points of Interest, *Mathematical Problems in Engineering*, 2012 (2012) 1-18.
- [18] D.-I. Curiac, C. Volosencu, A 2D chaotic path planning for mobile robots accomplishing boundary surveillance missions in adversarial conditions, *Communications in Nonlinear Science and Numerical Simulation*, 19 (2014) 3617-3627.
- [19] C. Li, Y. Song, F. Wang, Z. Liang, B. Zhu, Chaotic Path Planner of Autonomous Mobile Robots Based on the Standard Map for Surveillance Missions, *Mathematical Problems in Engineering*, 2015 (2015) 1-11.
- [20] C. Li, F. Wang, L. Zhao, Y. Li, Y. Song, An Improved Chaotic Motion Path Planner for Autonomous Mobile Robots Based on a Logistic Map, *International Journal of Advanced Robotic Systems*, 10 (2013).
- [21] C.H. Pimentel-Romero, J.M. Munoz-Pacheco, O. Felix-Beltran, L.C. Gomez-Pavon, C.K. Volos, Chaotic Planning Paths Generators by Using Performance Surfaces, in: *Fractional Order Control and Synchronization of Chaotic Systems*, 2017, pp. 805-832.
- [22] C. Li, Y. Song, F. Wang, Z. Wang, Y. Li, A Bounded Strategy of the Mobile Robot Coverage Path Planning Based on Lorenz Chaotic System, *International Journal of Advanced Robotic Systems*, 13 (2016).

- [23] C. Luo, X. Wang, Chaos in the fractional-order complex Lorenz system and its synchronization, *Nonlinear Dynamics*, 71 (2012) 241-257.
- [24] A. Sekiguchi, Y. Nakamura, Behavior Control of Robot Using Orbits of Nonlinear Dynamics, in: *Proceedings of the 2001 IEEE International Conference on Robotics & Automation*, IEEE, Seoul, Korea, 2001, pp. 1647-1652.
- [25] A. Zhu, L. Henry, Cooperation Random Mobile Robots Based on Chaos Synchronization, in: *Proceedings of International Conference on Mechatronics*, IEEE, Kumamoto, Japan, 2007, pp. 1-5.
- [26] C.K. Volos, I.M. Kyprianidis, I.N. Stouboulos, Experimental investigation on coverage performance of a chaotic autonomous mobile robot, *Robotics and Autonomous Systems*, 61 (2013) 1314-1322.
- [27] K. Sridharan, Z. Nili Ahmadabadi, A Multi-System Chaotic Path Planner for Fast and Unpredictable Online Coverage of Terrains, *IEEE Robotics and Automation Letters*, 5 (2020) 5268-5275.
- [28] J. Lu, G. Chen, D. Cheng, A new chaotic system and beyond: the generalized Lorenz-like system, *International Journal of Bifurcation and Chaos*, 14 (2004) 1507-1537.
- [29] C.K. Volos, N.G. Bardis, I.M. Kyprianidis, I.N. Stouboulos, Implementation of mobile robot by using Double-Scroll Chaotic Attractors, *Recent Researchers in Applications of Electrical and Computer Engineering*.
- [30] H.N. Agiza, M.T. Yassen, Synchronization of Rossler and Chen chaotic dynamical systems using active control, Elsevier, (2001).
- [31] D.K. Arrowsmith, J.H.E. Cartwright, A.N. Lansbury, C.M. Place, The Bogdanov Map: Bifurcation Mode, Locking and Chaos in a dissipative system, *International Journal of Bifurcation and Chaos*, 3 (1993) 808-842.
- [32] C. Li, Y. Song, F. Wang, Z. Wang, Y. Li, A chaotic coverage path planner for the mobile robot based on the Chebyshev map for special missions, *Frontiers of Information Technology and Electronic Engineering*, 18 (2017) 1305-1319.